Structure of molten trivalent metal chlorides studied by using neutron diffraction: the systems $TbCl_3$, YCl_3, $HoCl_3$ and $ErCl_3$

1999 J. Phys.: Condens. Matter 11 9293

(http://iopscience.iop.org/0953-8984/11/47/313)

J. Phys.: Condens. Matter **11** (1999) 9293–9302. Printed in the UK PII: S0953-8984(99)06789-2

Structure of molten trivalent metal chlorides studied by using neutron diffraction: the systems $TbCl_3$, YCl_3, $HoCl_3$ and $ErCl_3$

Jonathan C Wasse† and Philip S Salmon‡
School of Physics, University of East Anglia, Norwich NR4 7TJ, UK

Received 9 August 1999

Abstract. The total structure factors of the molten trivalent metal chlorides MCl_3, where M denotes Tb, Y, Ho or Er, were measured by using neutron diffraction. All four salts melt with a small volume change of $\leqslant$5% from structures comprising MCl_6^{3-} octahedra to form liquids which show intermediate-range ionic ordering as manifest by a first sharp diffraction peak at $\approx$1 Å^{-1} that moves to smaller scattering vector values with decreasing cation size. In the liquid state, the M–Cl distances are comparable with the sum of the ionic radii and the results are consistent with the existence of distorted MCl_6^{3-} octahedral units. The implications of the results for a polarizable ion interaction model used in recent molecular dynamics calculations are briefly discussed.

1. Introduction

The object of this paper is to present neutron diffraction results on the structure of the molten trivalent metal chlorides MCl_3 where M denotes Tb, Y, Ho or Er. The work forms part of a systematic experimental study to find the effect of ion size on the structure of molten trivalent metal chlorides and related compounds in which the liquid and amorphous materials diffractometer, LAD, has played a pivotal role (Wasse and Salmon 1998a, b, 1999a, b, Wasse 1998). Motivation for the research is provided by the observation that as the cation radius is reduced from La^{3+} to Al^{3+} a rich diversity is found in the crystal structures of these materials and in their behaviours on melting which is consistent with an increasing 'covalent' character. For example, $LaCl_3$ crystallizes in the UCl_3-type structure and melts at a high temperature with a volume change on melting $\Delta V/V_m$ of 16%, where $\Delta V = V_m - V_{RT}$; V_m is the molar volume of the liquid at the melting point temperature T_m and V_{RT} is the molar volume of the salt at room temperature (see table 1). By comparison, $AlCl_3$ crystallizes in the YCl_3-type structure and melts at a low temperature with a large volume change on melting of 46–48% into an insulating liquid that is thought to comprise Al_2Cl_6 dimers (Hutchinson *et al* 1999a). The MCl_3 systems therefore provide a sensitive test-bed for the development of interaction models in which effects often attributed to 'covalency' cannot be neglected (Tosi *et al* 1991, Madden and Wilson 1996, Hutchinson *et al* 1999a, b, Takagi *et al* 1999).

The systems involved in the present work comprise cations of size intermediate between La^{3+} and Al^{3+} and have correspondingly distinct properties. For instance, although YCl_3,

† Now at: Department of Physics and Astronomy, University College London, Gower Street, London WC1E 6BT, UK.
‡ Author for correspondence. Now at: Department of Physics, University of Bath, Bath BA2 7AY, UK.

0953-8984/99/479293+10$30.00

Table 1. The radius r_M for sixfold-coordinated cations (Shannon 1976), room temperature crystal structure, molar volume V_{RT}, cation chemical parameter χ_M (Pettifor 1986), melting point temperature T_m, entropy change on melting ΔS_m, volume change $\Delta V/V_m$ and electrical conductivity near the melting point κ_m of several MCl_3 systems.

Salt	r_M (Å)	Crystal structure	V_{RT} ($cm^3\ mol^{-1}$)	χ_M	T_m (°C)	ΔS_m ($cal\ K^{-1}\ mol^{-1}$)	$\Delta V/V_m$ (%)	κ_m ($\Omega^{-1}\ cm^{-1}$)
$LaCl_3$	1.03	UCl_3[a]	63.79[a]	0.705	858[b]	11.5[b]	16[c,d]	1.2–1.5[e,f]
$TbCl_3$	0.92	$PuBr_3$[g]	57.69[g]	0.6875	582[b]	5.4[h]	21[i]	—
YCl_3	0.90	YCl_3[j]	74.82[j]	0.66	714[k]	7.6[b]	0.6–3[k,l]	0.35–0.40[l,m]
$HoCl_3$	0.90	YCl_3[j]	73.02[j]	0.6825	720[b]	7.3[b]	1–3[n,o]	0.39[p]
$ErCl_3$	0.89	YCl_3[j]	72.11[j]	0.68	775[b,q]	7.1–7.4[b,q]	5[o,r]	0.3–0.4[p,s]
$AlCl_3$	0.54	YCl_3[j]	54.09[t]	1.66	193[h]	18.1[h]	46–48[u]	5.6×10^{-7} [l]

[a] Morosin (1968).
[b] Dworkin and Bredig (1971).
[c] Yaffe and van Artsdalen (1956).
[d] Igarashi and Mochinaga (1987).
[e] Janz *et al* (1975), Fukushima *et al* (1991).
[f] Gaune *et al* (1996).
[g] Forrester *et al* (1964).
[h] Pankratz (1984).
[i] See text.
[j] Templeton and Carter (1954).
[k] Mochinaga and Irisawa (1974).
[l] Klemm (1964).
[m] Mochinaga *et al* (1993).
[n] Iwadate *et al* (1995).
[o] Nisel'son and Lyzlov (1975).
[p] Janz *et al* (1968).
[q] Gaune-Escard *et al* (1994).
[r] Iwadate *et al* (1994).
[s] Fukushima *et al* (1995).
[t] *Landolt–Börnstein* (1973).
[u] Biltz and Voigt (1923), King and Seegmiller (1971).

$HoCl_3$, $ErCl_3$ and $AlCl_3$ all crystallize at room temperature into the YCl_3-type structure (Templeton and Carter 1954), unlike $AlCl_3$ the former salts melt at a high temperature with a small volume change into liquids with a substantial electrical conductivity (table 1). Furthermore, while the ionic radii of Tb^{3+}, Y^{3+}, Ho^{3+} and Er^{3+} are comparable (Shannon 1976), $TbCl_3$ crystallizes into the $PuBr_3$-type structure at room temperature (Forrester *et al* 1964). It then undergoes a solid–solid phase transition at 510 °C into a structure consisting of $TbCl_6^{3-}$ double octahedra (Gunsilius *et al* 1988) with an entropy change of 4.3 $cal^{-1}\ K^{-1}\ mol^{-1}$ (Pankratz 1984) and volume change $(V_{HT} - V_{RT})/V_{HT}$ of 21%, where V_{HT} is the molar volume of the high-temperature phase. It then melts at 582 °C with a small volume change on melting $(V_m - V_{HT})/V_m$ of 0.2% (Nisel'son and Lyzlov 1975). A solid–solid phase transition at 752 °C just below T_m with an entropy change of 1.2 $cal^{-1}\ K^{-1}\ mol^{-1}$ is also reported for $ErCl_3$ from differential scanning calorimetry experiments, although the structural character of this transition is unknown (Gaune-Escard *et al* 1994). Information from experiment on the structure of these particular melts is, however, scarce, being restricted to a neutron diffraction study on YCl_3 (Saboungi *et al* 1991) and an x-ray diffraction study on $ErCl_3$ (Iwadate *et al* 1994, 1995). Such information is, nevertheless, important to provide a benchmark test of, for example, recent computer simulation studies on MCl_3 systems, which use an ionic interaction model that includes an account of ionic polarization phenomena (Hutchinson *et al* 1999a, b).

2. Theory

In a neutron diffraction experiment on a molten MCl_3 salt comprising paramagnetic cations the differential scattering cross section per ion for unpolarized neutrons can be written as

$$\left(\frac{d\sigma}{d\Omega}\right)_{tot} = \left(\frac{d\sigma}{d\Omega}\right)_{mag} + \left(\frac{d\sigma}{d\Omega}\right)_{nucl}. \tag{1}$$

For the present materials, the rare-earth cations Tb^{3+}, Er^{3+} and Ho^{3+} exhibit paramagnetism and in the free ion approximation their paramagnetic differential scattering cross section $(d\sigma/d\Omega)_{mag}$ can be calculated by using the scheme outlined by Wasse and Salmon (1999a). The nuclear differential scattering cross section is given by

$$\left(\frac{d\sigma}{d\Omega}\right)_{nucl} = F(k) + \sum_{\alpha} c_\alpha [b_\alpha^2 + b_{inc,\alpha}^2][1 + P_\alpha(k)] \tag{2}$$

where the total structure factor is defined by

$$F(k) = A[S_{MM}(k) - 1] + B[S_{MCl}(k) - 1] + C[S_{ClCl}(k) - 1] \tag{3}$$

and $A = c_M^2 b_M^2$, $B = 2c_M c_{Cl} b_M b_{Cl}$, $C = c_{Cl}^2 b_{Cl}^2$. In these equations k denotes the magnitude of the scattering vector, c_α, b_α, $b_{inc,\alpha}$ give the atomic fraction, coherent scattering length and incoherent scattering length of chemical species α, $P_\alpha(k)$ is the inelasticity correction for chemical species α (Yarnell *et al* 1973, Howe *et al* 1989), and $S_{\alpha\beta}(k)$ is a Faber–Ziman partial structure factor. The total pair distribution function corresponding to the total structure factor is obtained by the Fourier transform relation

$$\begin{aligned} G(r) &= \frac{1}{2\pi^2 n_0 r}\int_0^\infty dk\, F(k) k \sin(kr) \\ &= A[g_{MM}(r) - 1] + B[g_{MCl}(r) - 1] + C[g_{ClCl}(r) - 1] \end{aligned} \tag{4}$$

where $g_{\alpha\beta}(r)$ denotes a partial pair distribution function and n_0 is the ionic number density of the melt. The values of the weighting coefficients in equations (3) and (4) are given in table 2 and were calculated using $b_{Tb} = 7.38(3)$ fm, $b_Y = 7.75(2)$ fm, $b_{Ho} = 8.01(8)$ fm, $b_{Er} = 7.79(2)$ fm and $b_{Cl} = 9.5770(8)$ fm (Sears 1992). The other scattering length and nuclear cross-section parameters used in the data analysis procedures were taken from Sears (1992). The mean number of particles of type β contained in a volume defined by two concentric spheres of radii r_i and r_j, centred on a particle of type α, is given by

$$\bar{n}_\alpha^\beta = 4\pi n_0 c_\beta \int_{r_i}^{r_j} r^2 g_{\alpha\beta}(r)\, dr. \tag{5}$$

Table 2. The weighting coefficients on the $S_{\alpha\beta}(k)$ and $g_{\alpha\beta}(r)$ functions.

Salt	A (mbarn)	B (mbarn)	C (mbarn)
$TbCl_3$	34.0(3)	265(1)	515.9(1)
YCl_3	37.5(2)	278.3(7)	515.9(1)
$HoCl_3$	40.1(8)	288(3)	515.9(1)
$ErCl_3$	37.9(2)	279.8(7)	515.9(1)

3. Experimental details

The $TbCl_3$ (99.99%), YCl_3 (99.99%), $HoCl_3$ (99.9%) and $ErCl_3$ (99.9%) salts, supplied by Aldrich, had a water content of less than 100 ppm. They were handled either in high vacuum or under a high-purity argon gas atmosphere having an oxygen and water content both less than 10 ppm. The YCl_3 was supplied in the form of beads while the other salts were supplied in powdered form and had to be pre-melted to increase their packing fraction. The salts were sealed under vacuum in cylindrical silica cells of 1 mm wall thickness, which had been cleaned using chromic acid and then etched with a 25% by mass solution of hydrofluoric acid, ready for the neutron diffraction experiments. The internal diameter of the cells was 5 mm for the $TbCl_3$, $HoCl_3$ and $ErCl_3$ samples and 7 mm for the YCl_3 sample.

The diffraction experiment on the YCl_3 sample was performed using the LAD instrument at the ISIS pulsed neutron source, Rutherford Appleton Laboratory, UK. This instrument was, however, not used for the other measurements owing to the presence of neutron absorption resonances in Tb, Ho and Er at unsuitable incident neutron energies (Mughabghab 1984). Instead, the diffraction experiments on the $TbCl_3$, $HoCl_3$ and $ErCl_3$ samples were performed using the SLAD instrument at the Studsvik reactor source, Sweden (Wannberg *et al* 1997) with an incident wavelength of 1.117(1) Å. Each complete experiment comprised the measurement of the diffraction patterns for the sample in its container in a cylindrical furnace, the empty container in the furnace, the empty furnace, and a vanadium rod of $\approx$8 mm diameter for normalization purposes. The LAD and SLAD data analyses were made using the ATLAS (Soper *et al* 1989) and CORRECT (Howe and McGreevy 1995) suite of programs respectively. The total paramagnetic cross-sections of the cations at the SLAD incident neutron wavelength were calculated by using the procedure described by Wasse and Salmon (1999a).

LAD comprises 14 groups of detectors at scattering angles of ±5, ±10, ±20, ±35, ±60, ±90 and $\pm150^\circ$ corresponding to instrumental resolution functions ($\Delta k/k$) of 11%, 6%, 2.8%, 1.7%, 1.2%, 0.8% and 0.5% respectively. SLAD comprises 12 horizontal position sensitive detectors which are arranged as four overlapping groups of three detectors spanning the scattering angle range $3^\circ \leqslant 2\theta \leqslant 135^\circ$ with a nominal resolution function ($\Delta k/k$) of 1% (Wannberg *et al* 1997). The final $F(k)$ were constructed by merging all those diffraction patterns from the different groups that showed good agreement. It was checked that the resultant $F(k)$ tend to the correct high-k limit, obey the usual sum rule relation, and that there is good overall agreement between $F(k)$ and the back-Fourier transform of the corresponding $G(r)$ after the unphysical low-r oscillations have been set to their calculated $G(0)$ limit (Salmon and Benmore 1992). The temperatures of the $TbCl_3$, YCl_3, $HoCl_3$ and $ErCl_3$ melts were 615(3) °C, 760(3) °C, 740(3) °C and 810(3) °C respectively. The corresponding number densities were estimated to be 0.0327(3) $Å^{-3}$ for $TbCl_3$ (Nisel'son and Lyzlov 1975), 0.0317(3) $Å^{-3}$ for YCl_3 (Mochinaga and Irisawa 1974), 0.0324(3) $Å^{-3}$ for $HoCl_3$ (Iwadate *et al* 1995, Nisel'son and Lyzlov 1975) and 0.0315(3) $Å^{-3}$ for $ErCl_3$ (Iwadate *et al* 1994). The full experimental details are given by Wasse (1998).

4. Results

The calculated paramagnetic differential scattering cross sections for Tb^{3+}, Er^{3+} and Ho^{3+} used in the data analysis are shown in figure 1 together with the total structure factors for molten $TbCl_3$, YCl_3, $HoCl_3$ and $ErCl_3$. There is a first sharp diffraction peak or pre-peak, which is a signature of intermediate-range ionic ordering in the melts (see e.g. Salmon 1994), at 1.01(4) $Å^{-1}$ for $TbCl_3$, 0.96(2) $Å^{-1}$ for YCl_3, 0.95(2) $Å^{-1}$ for $HoCl_3$ and 0.92(2) $Å^{-1}$

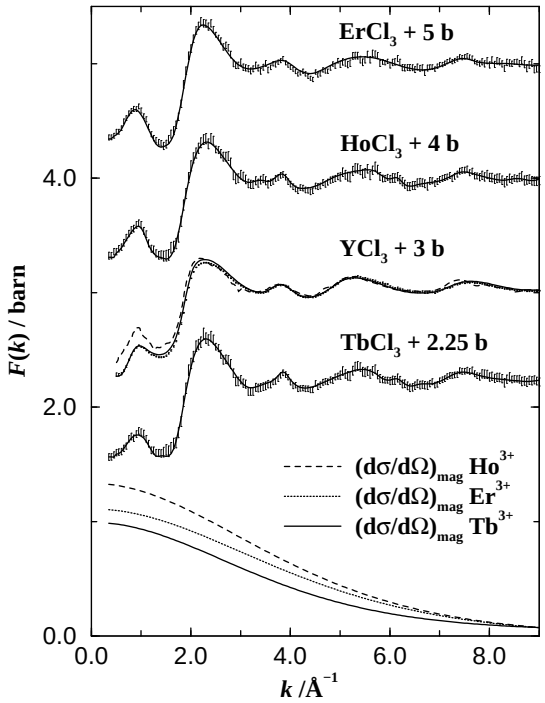

Figure 1. The measured total structure factor $F(k)$ for the liquids $TbCl_3$ at 615(3) °C, YCl_3 at 760(3) °C, $HoCl_3$ at 740(3) °C and $ErCl_3$ at 810(3) °C. The bars represent the statistical errors on the data points and the solid curves are the Fourier back-transforms of the corresponding $G(r)$ given by the solid curves in figure 2. The dashed curve gives the $F(k)$ measured for molten YCl_3 at 747 °C by Saboungi *et al* (1991). The calculated paramagnetic differential scattering cross sections $(d\sigma/d\Omega)_{mag}$ for Tb^{3+}, Ho^{3+} and Er^{3+} are also shown.

for $ErCl_3$. Hence the pre-peak position shifts to smaller k-values with decreasing cation size. The $F(k)$ for YCl_3 at 760 °C is in good agreement with that measured by Saboungi *et al* (1991) at 747 °C except in the low-k region, which may relate to a background correction problem. The pre-peak position is nevertheless the same at ≈ 0.95 Å^{-1}.

The corresponding $G(r)$ in figure 2 show a strong overlap between the first and second peaks. This overlap is accentuated in the case of the $TbCl_3$, $HoCl_3$ and $ErCl_3$ melts owing to the limited k-space range of $0.3 \leqslant k$ (Å^{-1}) $\leqslant 10.4$ that was accessible with the SLAD instrument. The diffraction pattern for YCl_3 was measured using LAD over an extended k-space range and gives correspondingly sharper peaks in $G(r)$ although it does not remove the peak overlap. This is illustrated in figure 2 where the effect on $G(r)$ of truncating $F(k)$ for YCl_3 at a node at ~ 9 Å^{-1} is compared with the effect of truncating $F(k)$ at 16 Å^{-1}. The benefit provided by the extended k-space range of LAD, when this instrument can be successfully applied, is thereby demonstrated.

The first peak in $G(r)$ for each melt (table 3) is assigned to M–Cl correlations by reference to the corresponding crystal structures and its position is comparable with the sum of the Shannon (1976) ionic radii for M^{3+} (table 1) and Cl^- (1.81 Å). By comparison with the crystal structures and in view of the large $g_{ClCl}(r)$ weighting factor C (table 2), the second peak in $G(r)$ will have a strong contribution from Cl–Cl interactions and is identified accordingly. The peak positions in $G(r)$ and the $\bar{n}_M^{Cl}$ coordination numbers, obtained by

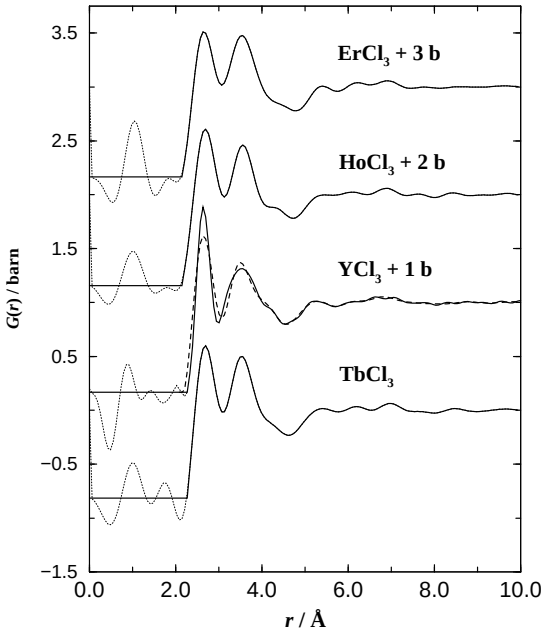

Figure 2. The total pair distribution function $G(r)$ for the liquids $TbCl_3$ at 615(3) °C, YCl_3 at 760(3) °C, $HoCl_3$ at 740(3) °C and $ErCl_3$ at 810(3) °C obtained by Fourier transforming the $F(k)$ given by the error bars in figure 1. The unphysical low-r oscillations about the $G(0)$ limits are shown by the broken curves. The dashed curve for molten YCl_3 shows the effect on $G(r)$ of truncating $F(k)$ at a node at ~ 9 Å^{-1} (see text).

Table 3. The local coordination environment of several molten MCl_3 salts.

Salt	Function	r_{MCl} (Å)	Integration range (Å)	$\bar{n}_M^{Cl}$	r_{ClCl} (Å)	$\bar{n}_{Cl}^{Cl}$
$TbCl_3$	$G(r)$	2.67(2)	7.5(2)	2.27(2)–3.05(2)	3.55(2)	—
	$r^2\{G(r) - G(0)\}$	2.72(3)	6.3(3)	—	3.58(3)	8.1(3)
YCl_3	$G(r)$	2.64(2)	6.2(2)	2.27(2)–2.95(2)	3.53(2)	—
	$r^2\{G(r) - G(0)\}$	2.72(3)	5.7(3)	—	3.55(3)	7.8(3)
$HoCl_3$	$G(r)$	2.69(2)	7.4(2)	2.15(2)–3.13(2)	3.56(3)	—
	$r^2\{G(r) - G(0)\}$	2.76(3)	6.4(3)	—	3.59(3)	8.1(3)
$ErCl_3$	$G(r)$	2.66(2)	6.7(2)	2.15(2)–3.07(2)	3.54(3)	—
	$r^2\{G(r) - G(0)\}$	2.74(3)	5.6(3)	—	3.58(3)	8.9(3)

integrating over the first peak in $G(r)$ to its first minimum using equation (5), are summarized in table 3.

In an attempt to refine the M–Cl coordination number and estimate the Cl–Cl coordination number, the first two peaks in the real space function $r^2\{G(r) - G(0)\}$ were fitted to a sum of Gaussians, representing the individual partial pair distribution functions, in the form

$$f(r) = \frac{1}{(2\pi)^{1/2}} \sum_{\beta} A_\beta \exp\{-(r - r_{\alpha\beta})^2/2\sigma_\beta^2\}/\sigma_\beta \tag{6}$$

where A_β, $r_{\alpha\beta}$ and σ_β are the area, mean position and standard deviation of Gaussian β. In this choice of fitting procedure the A_β are directly proportional to the coordination numbers $\bar{n}_\alpha^\beta$ (Lond *et al* 1991). The fitted data are shown in figure 3 and the fitted peak positions and coordination numbers are given in table 3.

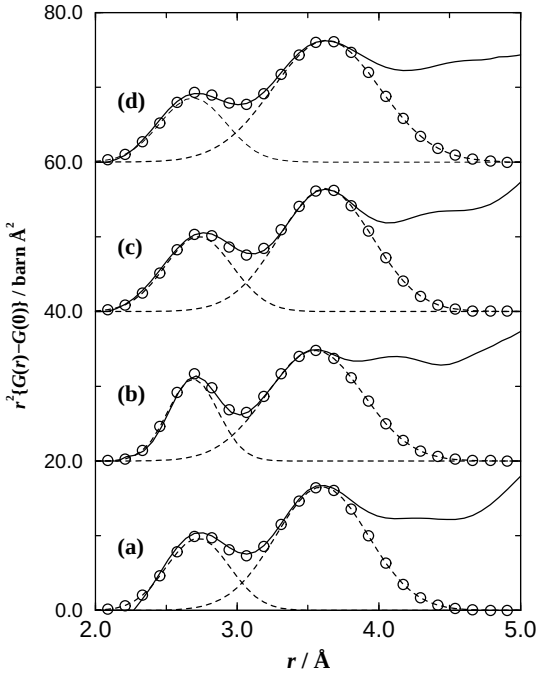

Figure 3. Fit to $r^2\{G(r)-G(0)\}$ by two Gaussians represented by the function $f(r)$ of equation (6): (a) $TbCl_3$; (b) YCl_3 (+20 barn Å^2); (c) $HoCl_3$ (+40 barn Å^2); (d) $ErCl_3$ (+60 barn Å^2). The solid curve gives the data, the open circles the fitted $f(r)$ and the broken curves the individual fitted Gaussians.

5. Discussion

For molten $TbCl_3$, $HoCl_3$ and $ErCl_3$ coordination numbers $\bar{n}_M^{Cl}$ of about seven are obtained by integrating over the first peak to the first minimum in $G(r)$ using equation (5). These are estimates owing to the overlap of the first two peaks in $G(r)$ which is accentuated by the peak broadening that results from the finite k-space measuring range of the SLAD instrument. In the case of molten YCl_3 truncating $F(k)$ at a value consistent with the SLAD high-k limit has the effect of increasing $\bar{n}_M^{Cl}$ from 6.2(2) to 6.4(2). The Gaussian fits to $r^2\{G(r)-G(0)\}$ give lower coordination numbers of $\bar{n}_M^{Cl} \approx 6$ within the experimental errors in accord with the octahedral coordination environment of the cation in the crystal structures of both YCl_3 (Templeton and Carter 1954) and the high-temperature phase of $TbCl_3$ (Gunsilius *et al* 1988). The measured nearest-neighbour Y–Cl parameters are in excellent agreement with the distance $r_{YCl} = 2.71$ Å and coordination number $\bar{n}_Y^{Cl} = 5.9$ obtained from previous neutron diffraction data on molten YCl_3 at 747 °C by a Gaussian fitting procedure to the function $T(r) \propto rG(r)$ (Saboungi *et al* 1991). A nearest-neighbour distance $r_{ErCl} = 2.63$ Å and coordination number $\bar{n}_{Er}^{Cl} = 5.8(2)$ were obtained from a previous x-ray diffraction study on molten $ErCl_3$ at 780 °C (Iwadate *et al* 1994).

The ratio of the nearest-neighbour peak positions r_{ClCl}:r_{MCl} for all of the melts, obtained from either $G(r)$ or $r^2\{G(r)-G(0)\}$ functions, is in the range 1.30–1.34 (table 3). This suggests a distortion of any MCl_6^{3-} conformations from regular octahedral geometry for which a ratio of $\sqrt{2}$ is expected. In molten YCl_3 the presence of distorted edge-sharing YCl_6^{3-} octahedra is supported by Raman spectroscopy experiments (Papatheodorou 1977). The $\bar{n}_{Cl}^{Cl}$

values obtained from the Gaussian fitting procedure to $r^2\{G(r) - G(0)\}$ are in good agreement with the values of 8.2 and 8–9 previously reported for molten YCl_3 (Saboungi *et al* 1991) and $ErCl_3$ (Iwadate *et al* 1994) respectively. The r_{ClCl} distances previously measured are, however, longer at 3.64 Å for YCl_3 and 3.75 Å for $ErCl_3$.

The $\bar{n}^{Cl}_{Cl}$ values measured for YCl_3, $HoCl_3$ and $ErCl_3$ are substantially less than the value of 12 found in the YCl_3-type crystal structure (Templeton and Carter 1954). This decrease has been attributed in YCl_3 (Saboungi *et al* 1991) to a break-down on melting of the local cubic close packing of the chloride ions in the solid phase (Müller 1993). Some reservations must, however, be placed on this viewpoint owing to the strong overlap of the peaks in $G(r)$ and the need to employ a fitting procedure to obtain coordination numbers. Nevertheless, in crystalline YCl_3 each chloride ion is surrounded by 12 other chloride ions in the range from 3.45 to 4.44 Å and each yttrium ion has three nearest-neighbour yttrium ions between 3.96 and 4.00 Å (Templeton and Carter 1954). The small $\Delta V/V_m$ implies that the liquid has a similar volume to the solid at room temperature which points to comparable nearest-neighbour inter-ionic separations. Integrating the area of the first two peaks in $G(r)$ for molten YCl_3 to the minimum at 4.54 Å and assuming $\bar{n}^{Cl}_{Y} = 6$ gives $\bar{n}^{Cl}_{Cl} = 10.4(2)$ if $\bar{n}^{Y}_{Y} = 0$ and $\bar{n}^{Cl}_{Cl} = 9.8(2)$ if $\bar{n}^{Y}_{Y} = 3$. There is, therefore, an apparent lowering of the Cl–Cl coordination number on melting. Further discussion of this problem requires information at the partial pair distribution function level whence, for example, running coordination numbers can be deduced.

In the high-temperature phase of $TbCl_3$ each chloride ion is surrounded by 13 other chloride ions in the range from 3.58 to 4.58 Å and each terbium ion has one nearest-neighbour terbium ion at 4.02 Å and four next nearest-neighbour terbium ions at 4.85 Å (Gunsilius *et al* 1988). The small volume change on melting of 0.2% points to comparable nearest-neighbour inter-ionic separations in both the high-temperature solid and liquid phases. Integrating the area of the first two peaks in $G(r)$ for molten $TbCl_3$ to the minimum at 4.60 Å and assuming $\bar{n}^{Cl}_{Tb} = 6$ gives $\bar{n}^{Cl}_{Cl} = 11.9(2)$ if $\bar{n}^{Tb}_{Tb} = 0$ and $\bar{n}^{Cl}_{Cl} = 11.7(2)$ if $\bar{n}^{Tb}_{Tb} = 1$. It is not therefore possible to argue for a clear reduction in the Cl–Cl coordination number on melting and, as in the case of molten YCl_3, partial pair distribution functions are required. In this context it will be interesting to make a detailed comparison of the molten $TbCl_3$ results with those for molten $DyCl_3$ for which measured $g_{\alpha\beta}(r)$ will soon become available (see Takagi *et al* 1999). $DyCl_3$ can crystallize into either the $PuBr_3$-type or YCl_3-type structure at room temperature (Bommer and Hohmann 1941, Templeton and Carter 1954, Forrester *et al* 1964) and a solid–solid phase transition has been reported with increasing temperature, albeit between unknown structures (Gaune-Escard *et al* 1994).

The present results for molten $TbCl_3$ and YCl_3 have recently been used to assess the ability of molecular dynamics simulations, using a polarizable formal charge ionic interaction model, to account for the properties of a range of trivalent metal chlorides from $LaCl_3$ to YCl_3 (Hutchinson *et al* 1999b). In these simulations the interaction model was a 'generic' one in the sense that the cation size was the only parameter used to distinguish one system from another. It was found that while the observed trends are reproduced, the simulated first coordination shell is more ordered than in experiment and there is also a difficulty in accounting for the Cl–Cl correlations. Hence there is a need to review the polarizable ion interaction model for trivalent metal chloride systems and the comparison between experiment and simulation suggests that particular attention should be paid to the short-ranged anion–anion interactions.

6. Conclusions

In summary, the $TbCl_3$, YCl_3, $HoCl_3$ and $ErCl_3$ systems all melt with a small volume change of $\leqslant 5\%$ to give liquids which have intermediate-range ionic ordering as manifest by the presence

of a first sharp diffraction peak in the measured total structure factors. The first two peaks in the corresponding real space functions show strong overlap and give M–Cl coordination numbers of about six for YCl_3 and seven for $TbCl_3$, $HoCl_3$ and $ErCl_3$. This coordination number for the latter three systems is reduced to about six on employment of a Gaussian fitting procedure, consistent with the survival into the liquid phase of the MCl_6^{3-} octahedral units that are the characteristic structural units of the high-temperature crystalline phases. The comparison made by Hutchinson *et al* (1999b) between the experimental and molecular dynamics results for molten MCl_3 systems highlights problems associated with the polarizable ion interaction model used in the simulations and thereby points the way forward for gaining new insight into these materials.

Acknowledgments

It is a pleasure to thank Paul Madden for his encouragement of the present work, Takeshi Usuki, Spencer Howells, John Dreyer and Duncan Francis for help with the LAD experiment, Robert Delaplane and Robert McGreevy for help with the SLAD experiments, Francis Hutchinson for useful discussions on MCl_3 systems and Chris Anson for help with the crystal structures. The EPSRC, CCP5 and EC TMR-LSF activity are thanked for financial support.

References

Biltz W and Voigt A 1923 *Z. Anorg. (Allg.) Chem.* **126** 39
Bommer H and Hohmann E 1941 *Z. Anorg. (Allg.) Chem.* **248** 373
Dworkin A S and Bredig M A 1971 *High Temp. Sci.* **3** 81
Forrester J D, Zalkin A, Templeton D H and Wallmann J C 1964 *Inorg. Chem.* **3** 185
Fukushima K, Ikumi T, Mochinaga J, Takagi R, Gaune-Escard M and Iwadate Y 1995 *J. Alloys Compounds* **229** 274
Fukushima K, Iwadate Y, Andou Y, Kawashima T and Mochinaga J 1991 *Z. Naturforsch.* a **46** 1055
Gaune P, Gaune-Escard M, Rycerz L and Bogacz A 1996 *J. Alloys Compounds* **235** 143
Gaune-Escard M, Rycerz L, Szczepaniak W and Bogacz A 1994 *J. Alloys Compounds* **204** 193
Gunsilius H, Borrmann H, Simon A and Urland W 1988 *Z. Naturforsch.* b **43** 1023
Howe M A and McGreevy R L 1995 *Internal Report NFL, Studsvik, Sweden* version 2.18
Howe M A, McGreevy R L and Howells W S 1989 *J. Phys.: Condens. Matter* **1** 3433
Hutchinson F, Rowley A J, Walters M K, Wilson M, Madden P A, Wasse J C and Salmon P S 1999b *J. Chem. Phys.* **11** 2028
Hutchinson F, Walters M K, Rowley A J and Madden P A 1999a *J. Chem. Phys.* **110** 5821
Igarashi K and Mochinaga J 1987 *Z. Naturforsch.* a **42** 777
Iwadate Y, Iida T, Fukushima K, Mochinaga J and Gaune-Escard M 1994 *Z. Naturforsch.* a **49** 811
Iwadate Y, Okako N, Koyama Y, Kubo H and Fukushima K 1995 *J. Mol. Liq.* **65–66** 369
Janz G J, Dampier F W, Lakshminarayanan G R, Lorenz P K and Tomkins R P T 1968 *Natl Bur. Stand. Ref. Data Ser.* **15** 1
Janz G J, Tomkins R P T, Allen C B, Downey J R Jr, Gardner G L, Krebs U and Singer S K 1975 *J. Phys. Chem. Ref. Data* **4** 871
King L A and Seegmiller D W 1971 *J. Chem. Eng. Data* **16** 23
Klemm A 1964 *Molten Salt Chemistry* ed M Blander (New York: Interscience) pp 535–606
Landolt–Börnstein New Series 1973 Group III, vol 7a, ed K-H Hellwege and A M Hellwege (Berlin: Springer) p 366
Lond P B, Salmon P S and Champeney D C 1991 *J. Am. Chem. Soc.* **113** 6420
Madden P A and Wilson M 1996 *Chem. Soc. Rev.* **25** 339
Mochinaga J, Fukushima K, Iwadate Y, Kuroda H and Kawashima T 1993 *J. Alloys Compounds* **193** 33
Mochinaga J and Irisawa K 1974 *Bull. Chem. Soc. Japan* **47** 364
Morosin B 1968 *J. Chem. Phys.* **49** 3007
Mughabghab S F 1984 *Neutron Cross Sections* vol 1 (Orlando, FL: Academic) part B
Müller U 1993 *Inorganic Structural Chemistry* (Chichester: Wiley)
Nisel'son L A and Lyzlov Yu N 1975 *Dokl. Akad. Nauk SSSR* **220** 608
Pankratz L B 1984 *Thermodynamic Properties of Halides* (Washington, DC: US Bureau of Mines) bulletin 674

Papatheodorou G N 1977 *J. Chem. Phys.* **66** 2893
Pettifor D G 1986 *J. Phys. C: Solid State Phys.* **19** 285
Saboungi M-L, Price D L, Scamehorn C and Tosi M P 1991 *Europhys. Lett.* **15** 283
Salmon P S 1994 *Proc. R. Soc.* A **445** 351
Salmon P S and Benmore C J 1992 *Recent Developments in the Physics of Fluids* ed W S Howells and A K Soper (Bristol: Hilger) p F225
Sears V F 1992 *Neutron News* **3** 26
Shannon R D 1976 *Acta Crystallogr.* A **32** 751
Soper A K, Howells W S and Hannon A C 1989 *Rutherford Appleton Laboratory Report* RAL-89-046
Takagi R, Hutchinson F, Madden P A, Adya A K and Gaune-Escard M 1999 *J. Phys.: Condens. Matter* **11** 645
Templeton D H and Carter G F 1954 *J. Phys. Chem.* **58** 940
Tosi M P, Pastore G, Saboungi M-L and Price D L 1991 *Phys. Scr.* T **39** 367
Wannberg A, Delaplane R G and McGreevy R L 1997 *Physica* B **234–6** 1155
Wasse J C 1998 *PhD Thesis* University of East Anglia, UK
Wasse J C and Salmon P S 1998a *Physica* B **241–3** 967
——1998b *J. Phys.: Condens. Matter* **10** 8139
——1999a *J. Phys.: Condens. Matter* **11** 1381
——1999b *J. Phys.: Condens. Matter* **11** 2171
Yaffe I S and van Artsdalen E R 1956 *Chem. Semi Ann. Prog. Rep. Oak Ridge Natl Lab.* **2159** 77
Yarnell J L, Katz M J, Wenzel R G and Koenig S H 1973 *Phys. Rev.* A **7** 2130